SIMULATION OF ORBITAL DEBRIS IMPACTS ON BUMPER SHIELDS*

Eugene S. Hertel, Jr.

Sandia National Laboratories, Albuquerque, New Mexico, U. S. A.

ABSTRACT

A series of numerical simulations have been performed using ***CTH*** to predict secondary debris formation and rear structure damage for typical bumper shields under a variety of impact geometries. The simulations span a range of velocities from ~3 to 12 km/s and are compared to the experiment data for the lower velocities (3 to 7 km/s). For one velocity (~7 km/s), ***CTH*** was used to demonstrate the effects of bumper thickness on secondary debris formation and rear structure damage. ***CTH*** was also used to simulate a 12 km/s impact of a sphere on a simple Whipple bumper shield and this result will be compared to analytic damage predictions at that velocity.

It has been found that ***CTH*** accurately predicts secondary debris propagation and rear structure damage for velocities throughout the experimentally accessible range. The ***CTH*** damage predictions at 12 km/s result in a higher ballistic limit than would be predicted from the analytic techniques.

1. INTRODUCTION

It is well known that the principal threat to orbiting space structures results from impact damage caused by orbiting space debris. Presently, conventional laboratory facilities can evaluate damage mechanisms or the effectiveness of protective structures against this debris at the lowest impact velocities expected in space. Analytic methods (Refs. 1, 2, and 3) for predicting impact damage have been used extensively to date. These analytic techniques generally consist of a fit-to-data at experimentally accessible velocities (less than ~7.5 km/s) and then extrapolation to higher velocities based on scaling theory. Simulations (Refs. 4 and 5) of impact events have also been used to estimate impact damage. These techniques have progressed to the point of providing realistic damage assessments, although, the analyses or models have not been validated over the velocity range of 7 to 12 km/s, primarily due to lack of experimental capabilities to launch the prerequisite size particles over that velocity range. However, recently developed capabilities are being used to evaluate simple shielding concepts at these velocities.

A requirement for an effective debris shield is that it must protect the spacecraft from impacts both from the micrometeoroid and orbital debris environment. The micrometeoroid environment is thought to result from dust-size particles having an average velocity of 20 km/s, while the orbital debris environment is believed to be millimeter or centimeter size particles weighing approximately a gram with average velocities of 10 km/s. It is generally assumed that the average density of the orbital debris environment is ~2.8 gm/cm^3, and therefore can be represented by the material properties of aluminum. The orbital debris environment, which is man-made space debris, is more hazardous than the micrometeoroid environment because of its relatively large mass and particle size. This makes the design requirements for an adequate bumper shield difficult to establish. This also places the critical portion of the velocity spectrum in a region outside of conventional experimental techniques.

Experimental techniques have been widely used at velocities below ~7.5 km/s. In addition, the experimental database has been extrapolated using scaling laws to the velocity regime not currently accessible. A combination of the two techniques has been used to design the debris shields that are expected to be used for upcoming long duration space vehicles. Both of these methods have short-comings. Due to difficulties in separating sabots from projectiles, the low velocity data is almost completely composed of spherical projectiles impacting bumper shields. Very little direct data exists at higher velocities, where current ballistic limits above ~7 km/s consist of scaling extrapolations from the spherical projectile impacts at 6-7 km/s. These extrapolations are made even though basic physical phenomena change as the velocity increases, even though the actual debris shapes may not be spherical.

The use of simulation tools allows us to perform numerical experiments that are not easily tractable in the laboratory. These techniques allow for variations in projectile shape, orientation, and velocity with minimal difficulty. Velocity can be varied over a wide range if the equation-of-state is capable of modelling the appropriate phase changes. Even though we do not consider these techniques to be fully validated for all problems of interest to the orbital debris community, they have been shown to replicate most important features of high- and hyper-velocity impacts.

* This work performed at Sandia National Laboratories supported by the U. S. Department of Energy under contract DE-AC04-76DP00789 with partial funding from NASA, Johnson Space Center.

lowed to increased in size for radii greater than 2.0 cm. The cell size in the region of interest was 0.025 × 0.025 cm. The computational resolution effectively limits the minimum fragment size that ***CTH*** will represent in its graphical output. However, smaller fragments are represented by ***CTH*** internally and will cause damage when striking other objects. An example of this phenomena can be seen in Figure 1.

Figure 1 displays the debris cloud at 10 μs after initial impact. The left side of the figure shows the material density in a *mirrored, dot-density* format, the *dot-density* legend is included with the figure. The right side of the figure shows only the material interfaces for the same axi-symmetric representation of experiment a1347. The material interfaces are simply contour lines (value 0.5) of the volume fractions for the materials in the simulation. On the left side of the figure, you can see (note A) where material is located by the density but is not represented by a material interface on the right side. This indicates that the fragments are smaller than a computational cell and no contour line of volume fraction can be drawn.

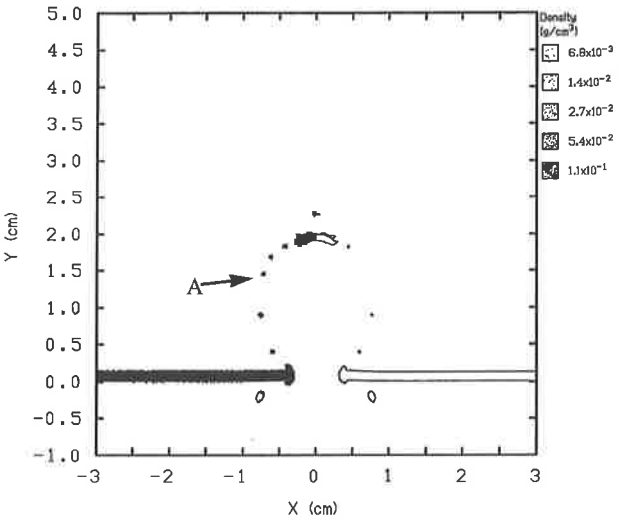

Figure 1. Baseline CTH debris formation for a1347.

Since the ability of ***CTH*** to represent small debris fragments is strongly influenced by the computational resolution, a variation on the baseline simulation was completed to assess the effects of cell size on the initial debris cloud structure. The cell sizes were decreased from 0.025 × 0.025 cm to 0.01 × 0.01 cm for a small region behind the bumper. The high resolution simulation was also run to 10 μs for comparison with the baseline. The higher resolution simulation is shown in Figure 2.

The baseline simulation was run to 60 μs and the rear sheet damage results are displayed Figure 3.

Figures 4 and 5 display the front and rear view of the recovered second sheet from experiment a1347. The back side photograph shows a detached spall bubble ~0.6 cm in diameter with a single perforation ~0.05 cm in diameter. The ***CTH*** simulation predicts (see Figure 3) spall with a diameter of 0.45 cm, but does not predict perforation. If the high resolution simulation was extended to allow for secondary impact, the damage would increase. The high resolution simulation predicts a narrower debris cloud which would lead to more mass (at roughly the same velocity) striking the second sheet near the centerline with greater damage. In addition, the perforation could develop relatively late in time due to structural response. For this simulation, the qualitative agreement between ***CTH*** and the experiment is very good, given the resolution limitations.

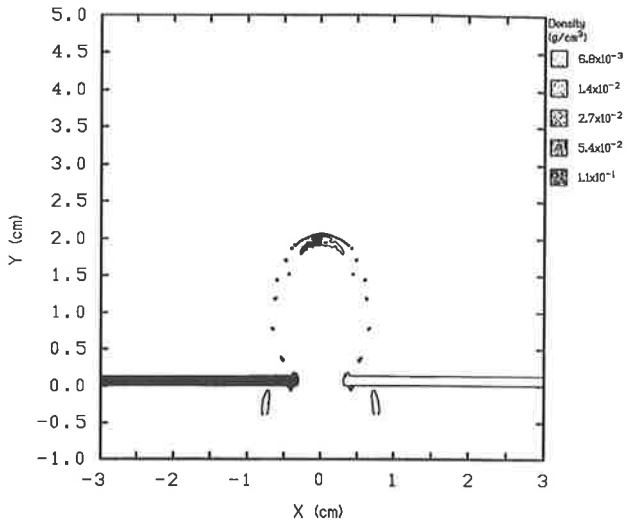

Figure 2. High resolution ***CTH*** debris formation for a1347.

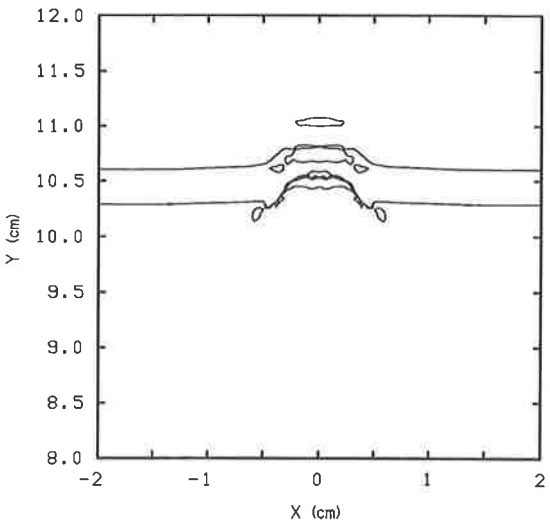

Figure 3. ***CTH*** rear sheet damage predictions for a1347.

3.2. b71

In this calculation, the zoning was square in the region of initial impact, throughout the debris propagation region, and at the rear wall. The radial zoning was allowed to increase in size for radii greater than 2.0 cm. The cell size in the region of interest was 0.015 × 0.015 cm. Figure 6 displays the terminal damage to the second sheet after 20 μs. At this time, a ~0.5 cm diameter perforation exists with an indication that a larger (~1 cm) plug could dislodge at late times. The ***CTH*** results were examined in detail and internal damage was evident at ~0.5 cm radius. At later times, this damage could lead to failure and a larger perforation estimate. Extensive damage on the back side of the second sheet has occurred over a 4-5 cm diameter and would indicate the possibility of a ~4 cm diameter spall region. The experimental data indicates a ~1.1 cm diameter hole with ~3.7 cm of detached spall diameter. Again, the agreement between ***CTH*** and the experiment is good.

The remaining sections of this paper will consist of a short overview of the ***CTH*** shock physics code and the results from four simulations of orbital debris impact events. Three of the four simulations are low velocity impacts and the ***CTH*** results are compared to the experimental data. The impact velocity of the final simulation is an extrapolation beyond current capabilities and that result is compared to the analytic extrapolation.

2. *CTH* OVERVIEW

The ***CTH*** (Ref. 6) code was developed to model a wide range of solid dynamics problems involving shock wave propagation and material motion in one, two, or three dimensions: one-dimensional rectilinear, cylindrical, and spherical meshes; two-dimensional rectangular and cylindrical meshes; and three-dimensional rectangular meshes are available. A two-step Eulerian solution scheme is used with these meshes. The first step is a Lagrangian step in which the cells distort to follow the material motion. The second step is a remesh step where the distorted cells are mapped back to the original Eulerian mesh. ***CTH*** has several thermodynamic models that are used for simulating strong shock, large deformation events. Both tabular and analytic equations-of-state are available. ***CTH*** can model material strength, high explosive detonation, fracture, and motion of fragments smaller than a computational cell. Material strength can be modelled as linearly-elastic perfectly-plastic, viscoplastic (strain rate dependent), or with two different brittle failure models. High explosive detonation can be modelled with a programmed burn model, or two different reactive burn models. A special model is available for moving fragments smaller than a computational cell with the correct statistical velocity. ***CTH*** has been carefully designed to minimize the dispersion generally found in Eulerian codes. It has a high-resolution interface tracker that prevents breakup and dispersion generally found in Eulerian codes. In addition, ***CTH*** uses a second-order convection scheme to flux all quantities between cells.

3. *CTH* SIMULATIONS

Four ***CTH*** simulations have been completed as a part of this study. The simulations use the Whipple (Ref. 7) bumper shield concept of a relatively thin (bumper thickness/projectile diameter << 1) front sheet that fragments, melts, and/or vaporizes the incoming projectile. The debris cloud then traverses a relatively large (separation/projectile diameter >> 1) void space prior to striking a back plate. If the Whipple shield is effective, the composite thickness of the front and back plate are less than the thickness of a single plate with equivalent stopping capabilities. Table 1 lists the impact and material parameters of the four simulations. Table 2 lists the yield and tensile strengths and densities for the four aluminum alloys required for the simulations. The values chosen for these simulations were not taken from a specific reference, but were chosen based on the collective experience of several analysts and are felt to be appropriate for the simulations. The values that were used reflect the well known increase in yield and fracture strength in a dynamic loading environment (Ref. 8).

The projectile and bumper were represented by the equation-of-state developed by Kerley (Ref. 9) and validated against experimental data for pressures below 80 GPa. The 2219-T87 and 2017-T4 forms of aluminum were also represented by the same equation-of-state with an adjustment made to reflect the higher initial density of those forms of aluminum. This form of the equation-of-state for aluminum is considered to be one of the best available to represent the solid-liquid and liquid-vapor phase changes.

The first two simulations were only compared to the terminal experimental data in the form of the damaged front and rear sheets. The comparison data for the third simulation consisted of radiographs of the debris cloud after impact with the front sheet. The last comparison actually consisted of several calculations. The ballistic limit was predicted for a 12 km/s normal impact and compared to the Cour-Palais (Ref. 2) analytic extrapolation for identical impact conditions.

3.1. a1347

The axi-symmetric geometry option was selected for this and the remaining ***CTH*** models. For this simulation, the zoning was square in the region of initial impact, throughout the debris propagation region, and at the rear wall. The radial zoning was al-

Model ID	Front Sheet Thickness (cm)	Second Sheet Thickness (cm)	Spacing (cm)	Projectile Diameter (cm)	Impact Velocity (km/s)
a1347	0.1270 (2)*	0.3175 (3)	10.16	0.358 (4)	2.93
b71	0.1270 (2)	0.2540 (4)	10.16	0.635 (4)	6.77
na1290	0.0305 (1)	0.6350 (2)	20.32	0.953 (4)	6.67
n12	0.1270 (2)	0.3175 (3)	10.16	0.840 (1) 0.820 (1)	12.0

Table 1. Bumper shield and projectile parameters for the ***CTH*** simulations.
* The numbers in parentheses refer to the material type as defined in Table 2.

Aluminum Type	Static Yield (dynes/cm^2)	Dynamic Yield (dynes/cm^2)	Fracture Strength (dynes/cm^2)	Density (gm/cm^3)	Material Number
1100-O	3.4×10^8	1.0×10^9	1.0×10^9	2.712	1
6061-T6	2.8×10^9	5.0×10^9	11.0×10^9	2.712	2
2219-T87	3.9×10^9	7.0×10^9	15.0×10^9	2.851	3
2017-T4	2.2×10^9	4.0×10^9	15.0×10^9	2.796	4

Table 2. Material parameters for the ***CTH*** simulations.

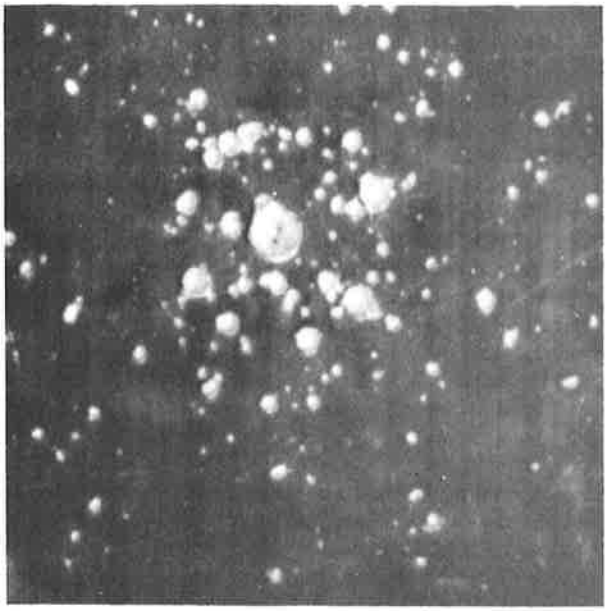

Figure 4. Experimental (front view) second sheet damage for a1347.

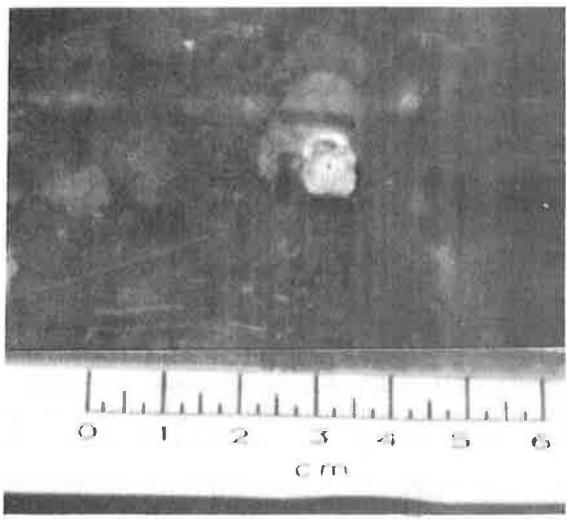

Figure 5. Experimental (rear view) second sheet damage for a1347.

3.3. na1290

The ***CTH*** simulation of an experiment done at the University of Dayton Research Institute (Ref. 10) is considered here. The experiment consists of a 0.9525 cm sphere impacting a 0.03048 cm front sheet at ~6.7 km/s. This simulation is similar to the one described above in that the impact velocities are nearly identical. However, significant differences exist in the dynamics of the debris formation due to the change in the thickness of the front sheet.

For this simulation, the zoning was square in the region of initial impact, throughout the debris propagation region, and at the rear wall. The radial zoning increased in size after the inner 3.0 cm. The cell size in the region of interest was 0.01 × 0.01 cm. To reduce the computational complexity of the simulation, a Galilean transformation was applied to the computational domain after the projectile perforated the front sheet. This was accomplished by adding an axial velocity of -6.5 km/s for 20 μs. This effectively removes 13.0 cm from the spacing between the front and rear sheets by causing the debris cloud to appear stationary for 20 μs.

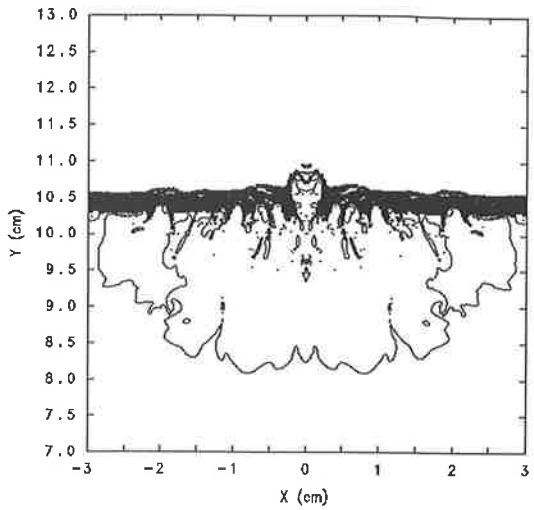

Figure 6. ***CTH*** rear sheet damage predictions for b71.

The use of this option is a commonly employed trick and does not change the basic nature of the simulation. However, it can significantly reduce the computational requirements to complete this and similar simulations.

Figure 7 displays the ***CTH*** predicted debris cloud as represented by a "cross-section" of the density at 10 μs. Figure 8 displays the

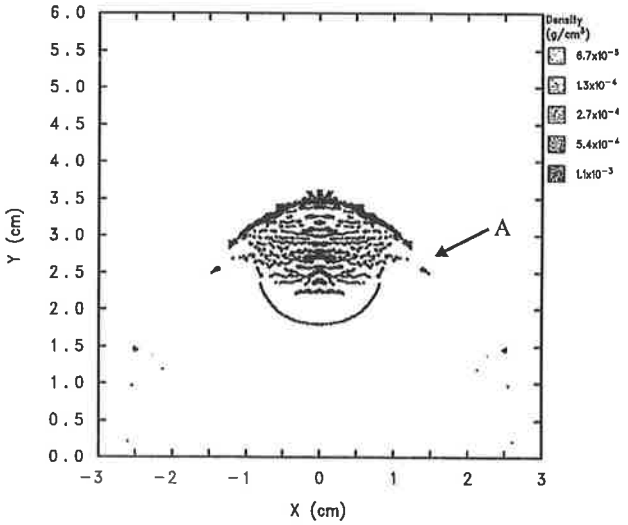

Figure 7. ***CTH*** debris cloud prediction for na1290.

experimental radiograph at approximately the same time. A comparison of the two figures shows remarkable similarity between the predicted results and experimental data. The image density as represented by the radiograph is proportional to the sum of material density along the line-of-sight. This makes a detailed comparison of the radiograph and the simulation results somewhat more difficult. From an investigation of the simulation results, one can determine that the leading edge (see A) of material is composed of very low density (~0.01 gm/cm^3) front sheet aluminum that is probably vaporized. The remainder of the debris cloud consists of fragmented projectile with some liquid droplets interspersed in the solid fragments. The simulation does an excellent job of matching the overall shape and mass distribution of the experimental debris cloud. The radiograph indicates a triangular shaped mass concentration near the center of the cloud. This feature is not well replicated by the "cross-section" plot of Figure 7. As

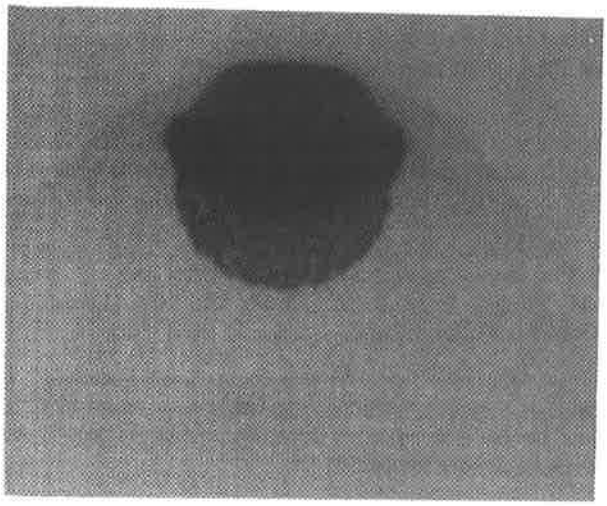

Figure 8. Experimental radiograph for na1290.

with the previous simulations, the agreement with the experimental results is good.

3.4. n12

The final simulation consisted of a series of impacts with varying projectile diameters. Table 1 lists the bumper shield configuration utilized for the simulations. The zoning was square in the region of initial impact with cell sizes 0.015 × 0.015 cm. The radial zoning increased in size after the inner 2.0 cm. The axial zoning was also increased in size 2.0 cm after the initial impact point. In the vicinity of the second sheet, the aspect ratio of the computational cells was 5:1. The projectile diameter was increased until ***CTH*** predicted a perforation of the second sheet by the debris cloud. These results were compared to the Cour-Palais analytical prediction (Ref. 2) of the ballistic limit for a two-sheet system.

The simulations indicate that perforation of the second sheet occurs at a projectile diameter of 0.84 cm for a 12.0 km/s impact velocity. For the same configuration, the analytical prediction of the ballistic limit is 0.52 cm. This result is displayed in Figure 9.

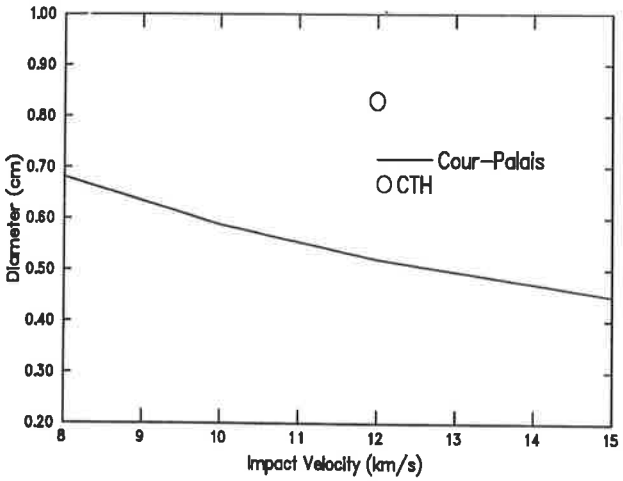

Figure 9. Ballistic limit comparison.

The ***CTH*** prediction is significantly above the analytical prediction for otherwise identical conditions. From an inspection of the ***CTH*** results, it is evident that the debris generated upon initial impact is predominately vapor. In addition, significant lateral dispersion is predicted for the debris. Under these circumstances, potential damage to the second sheet is reduced. Since the simulations are relatively short (~20 μs), the possibility for late time structural failure has not been considered. The analytical scaling techniques used in the Cour-Palais and other approximations take into account late time (structural) as well as short time (prompt shock) phenomena. The question of time domains may be one of the principal sources of difference between the ***CTH*** and analytical predictions of the ballistic limit. Appropriate experimental data at impact velocities above 10 km/s is necessary to understand the discrepancies.

4. CONCLUSIONS

CTH was used to predict the response of a two-sheet Whipple-type orbital debris shields for four different impact configurations. The impact velocities ranged from ~3 to 12 km/s with projectile diameters of ~0.4 to ~1.0 cm. Three of the four simulations were compared to experimental data generated at NASA Johnson Space Center and the University of Dayton Research Institute. The fourth simulation was beyond the range of current experimental techniques and was contrasted with analytical predictions. The comparisons were made on the basis of damage to the second sheet and with the structure of the debris cloud generated by the initial impact.

The simulation of experiment a1347 results in a debris cloud composed of solid fragments. The computational resolution chosen has a small affect on the relative mass distribution in the debris cloud, but not on the overall shape. The low resolution simulation predicts significant damage to the second sheet but does not predict perforation. The size of the impact crater and rear spall diameter is well correlated with the experimental results. The differences in the perforation prediction could be due to two causes: (1) the perforation could be due to late time failure that was not replicated in the time domain of the simulation; (2) a comparison of the low and high resolution debris cloud simulations indicates that higher resolution for the remainder of the simulation concentrates more mass at the secondary impact location and could lead to more damage and perforation.

The simulation of experiment b71 again results in a debris cloud composed of solid fragments with some molten material interspersed. The simulation predictions for the damage, perforation size, and second sheet spall are well correlated with the experimental data. The initial perforation diameter is ~0.5 cm with a strong indication that late time dynamics will result in a ~1.0 cm perforation, which is in excellent agreement with the experimental result of 1.1 cm. However, a longer simulation should be completed to remove the uncertainties in perforation diameter.

The simulation of experiment na1290 results in a debris cloud composed of solid and molten fragments with some vaporized material leading the debris cloud. From an inspection of the results one can determine that the shock-vaporized material is composed of front-sheet aluminum. Even though the impact velocities of na1290 and b71 are similar (6.67 to 6.77 km/s), the structure of the debris clouds from the initial impacts are significantly different. The differences are due to the relative differences in the thickness of the front sheet to the projectile diameter. These thickness differences cause a significant difference in the dynamics of the initial impact. A comparison of the predicted debris cloud with the experiment again reveals very good correlation of key features. The size and shape of the experimental debris cloud is matched almost exactly by the ***CTH*** simulation. Some internal features of the radiograph are not matched, prima-

rily due to the differing information available in the simulation.

The final simulation consisted of an attempt to computationally determine the ballistic limit for a two-sheet Whipple system at 12.0 km/s. The ***CTH*** simulations predicted a significantly higher (0.83 to 0.52 cm) ballistic limit than would have been expected from the current analytic approximations. For this velocity, the simulations predict a significant amount of vaporization of the debris cloud due to the initial impact. It is the amount of vapor production that causes the increase in the ballistic limit, four times the mass (as compared to the Cour-Palais approximation) is required to perforate the second sheet at 12.0 km/s. There have been attempts at validation of ***CTH*** at velocities above ~7 km/s (Refs. 4 and 12). The results of these experimental comparisons lend credence to the validity of the ***CTH*** ballistic limit prediction, however, further validation in this velocity range should be completed.

In general, ***CTH*** has been found to accurately predict the key features of low to medium velocity impacts on two-sheet systems. ***CTH*** has also been used to predict the impact dynamics at velocities above the experimentally accessible range and differs significantly with analytic extrapolations for the same conditions.

REFERENCES

1. J. P. D. Wilkinson, "A Penetration Criterion for Double-Walled Structures Subject to Meteoroid Impact," AIAA Journal, Vol. 7, pp. 1937-1943, 1969.

2. B. G. Cour-Palais, "Meteoroid Protection by Multiwall Structures," AIAA Paper No. 69-372, Proceedings of the AIAA Hypervelocity Impact Conference, 1969.

3. E. L. Christiansen, "Shield Sizing and Response Equations," NASA Johnson Space Center Technical Note SN3-91-42, 1991.

4. E. S. Hertel, Jr., L. C. Chhabildas, and S. A. Hill, "Whipple Bumper Shield Simulations," in Shock Waves in Condensed Matter-1991, edited by S. C. Schmidt, J. W. Jorbes, and R. D. Dick, Elsevier Science Publishers B. V., 1992.

5. L. C. Chhabildas and E. S. Hertel, Jr., "Comparison of Analytic Whipple Bumper Shield Ballistic Limits with CTH Simulations," Sandia National Laboratories SAND92-0347, September 1992.

6. J. M. McGlaun, S. L. Thompson, L. N. Kmetyk, and M. G. Elrick, "A Brief Description of the Three-Dimensional Shock Wave Physics Code CTH," Sandia National Laboratories SAND89-0607, July 1990.

7. F. L. Whipple, "Meteoric Phenomena and Meteorites," in Physics and Medicine of the Upper Atmosphere, edited by C. S. White and O. O. Benson, Jr., University of New Mexico Press, Albuquerque, New Mexico, 1952.

8. J. R. Asay, L. C. Chhabildas, G. I. Kerley, and T. G. Trucano, "High Pressure Strength of Shocked Aluminum," in Shock Waves in Condensed Matter-1985, edited by Y. M. Gupra, Plenum Publishers, 1986.

9. G. I. Kerley, "Theoretical Equation of State for Aluminum," Int. J. Impact Engng., Vol 5, pp. 441-449, 1987.

10. A. J. Piekutowski, "Properties of Largest Fragment Produced by Hypervelocity Impact of Aluminum Spheres with Thin Aluminum Sheets," Space Programs and Technologies Conference, AIAA Paper #92-1588.

11. E. S. Hertel, Jr., "Comparison of Analytic Whipple Bumper Shield Ballistic Limits with CTH Simulations," Sandia National Laboratories SAND92-0347, September 1992.